Experimental and Numerical Study on Behaviour of Model Sheet Pile Foundation Subjected to Vertical and Horizontal Loading

Wentao Guo [i), ii)], Takumi Kosaka [i)], Xi Xiong [i)], Tatsunori Matsumoto [i)] and Yukihiro Ishihara [iii)]

i) Kanazawa University, Department of Environment Design, Kakuma, Kanzawa 920-1192, Japan.

ii) Datang Carera Investment Co., LTD, No. 40, Xueyuan Rd., Haidian District, Beijing 100035, China.

iii) GIKEN LTD, Nunoshida, Kochi-shi, Kochi 781-5195, Japan

ABSTRACT

In recent years, efficient installation methods of piles have been developed. Nowadays, a challenge in piling engineering is to reduce costs including transportation and construction costs, and at the same time to keep safety of foundation structures. Hence, a target in this research is to show a possibility to use steel sheet piles for permanent piled raft foundations, because time and cost of construction of sheet piles could accurately be lower than those of pipe piles. In this study, a series of model tests were conducted first to investigate the load transfer behaviours of model foundations supported by three different types piles in dry sand ground subjected to vertical and horizontal loading. Then, corresponding numerical analyses of model tests on sheet piles were conducted using a three-dimensional finite element program PLAXIS 3D. According to the test and calculated results, a sheet pile foundation would be a promising alternative to conventional pipe pile foundation, especially in high-seismic areas.

Keywords: pile foundation, load test, sand ground, FEM simulation

1 INTRODUCTION

The piled raft foundation is one of the most important foundation structures that support the superstructure. Generally, the shape of the pile is a round cylinder (hereinafter referred to as a pipe pile). In recent years, efficient installation methods of piles have been developed (eg. Proc. of the 1st Int. Conf. on Press-in Eng., 2018), such as Silent Piler and Gyro Piler etc. Using these technologies, sheet piles, a kind of plate-shaped pile, can be installed with high accuracy and high-quality.

Owing to this background, a sheet pile foundation has been proposed as a new foundation type (Punrattanasin et al. 2002). In this paper, a series of experimental and numerical studies were conducted to show the possibility to use steel sheet piles for piled raft foundations of a permanent structure.

2 EXPERIMENTAL DESCRIPTION

2.1 Model ground

The sand used as model ground was air-dried Silica sand #6. Table 1 shows the physical properties of the sand. The model ground was prepared in a rectangular box with dimensions of 500 mm in width × 800 mm in length × 530 mm in height. The model ground was prepared with 10 layers of 50 mm thick and one top layer of 30 mm thick. The sand of each layer was poured into the soil box and compacted by hand tamping to get a target relative density, D_r = 82% (ρ_d = 1.533 ton/m^3).

Table 1. Physical properties of Silica sand #6 (after Vu et al, 2018).

Property	Value
Soil particle density, ρ_s (ton/m^3)	2.679
Minimum dry density, ρ_{dmin} (ton/m^3)	1.268
Maximum dry density, ρ_{dmax} (ton/m^3)	1.604
Maximum void ratio, e_{max}	1.089
Minimum void ratio, e_{min}	0.652
Model ground relative density, D_r (%)	82.5
Model ground density ρ_d (ton/m^3)	1.533

2.2 Model foundations

The model piles used in all experiments were made of aluminum round pipes and plates. The plates were used to represent sheet piles. Three different types of

model pile foundations were used in the experiments, as shown in Fig. 1. The first one is a foundation supported by open-ended pipe piles with an outer diameter of 20 mm, an inner diameter of 17.2 mm, a wall thickness of 1.4 mm and a length of 210 mm (called OPF, Fig. 1a). The 2nd is a foundation supported by plate piles with a width of 40 mm, a length of 195 mm and a thickness of 2 mm (called PPF, Fig. 1b). The 3rd is the one supported by box-shaped pile with a width of 40 mm, a length of 195 mm and a thickness of 2 mm (called BPF, Fig. 1c). The geometrical and mechanical properties of the model piles are listed in Table 2.

It was intended to use the same volume of pile material for the three model foundations with the same length. Note that one BP was used, while 4 OPs or 4PPs were used. Hence, the total volume of piles of each foundation was almost same, as shown in Table 2.

As shown in Fig. 1, fourteen strain gauges were attached on opposite sides of each pile of PP and OP. And eighteen strain gauges were attached on sides of BP.

The model square raft had a side length of 100 mm and a thickness of 30 mm, as shown in Fig. 1. Pile heads were rigidly connected to the raft in all the foundations.

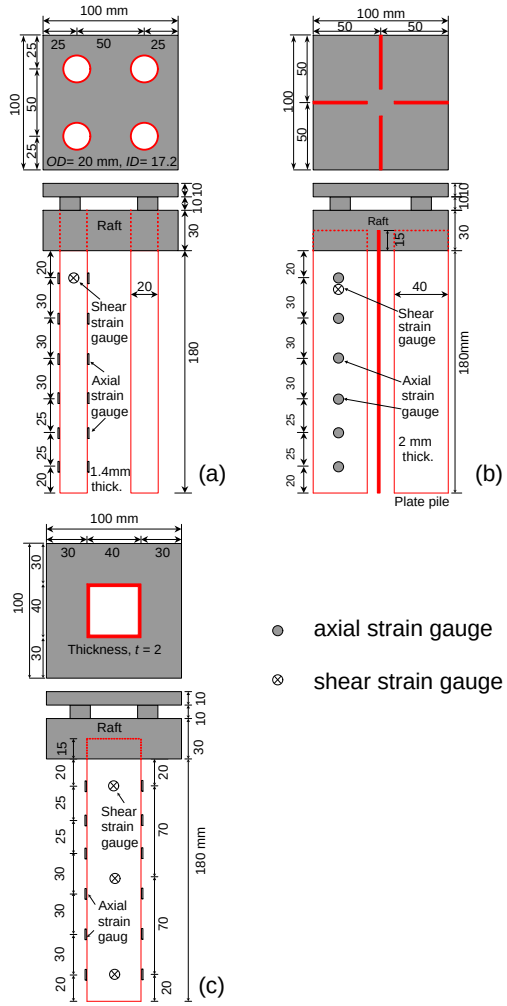

Fig. 1. Model pile foundations: (a) Pipe pile foundation; (b) Plate pile foundation; (c) Box pile foundation.

Table 2. Geometrical and mechanical properties of the model pile.

	OP	PP	BP
Length from raft base, L (mm)	180	180	180
Cross sectional area, A (mm)	81.8	80	304
Wall thickness, t (mm)	1.4	2	2
Young's modulus, E (GPa)	71.3	69.5	75.6
Poisson's ratio, ν	0.343	0.297	0.356
Bending rigidity, EI (MNmm^2)	253.7	1.85	5546.1
Bending rigidity, EI (MNmm^2) (Strong axis)	-----	742	-----

2.3 Test devices and instrumentation

Fig. 2 shows test devices and instrumentation used in model tests. During the load tests, the vertical load was applied by a screw jack and the horizontal load by a winch (Fig. 2). And the horizontal load applied to the foundation was measured utilizing a load cell attached between the raft and the winch. Horizontal displacement and vertical displacements of the raft were measured utilizing dial gauges (Fig. 2). And the inclination of the raft was obtained from an inclinometer.

It is noticed that the inclination of the pile top was equal to the raft inclination as the piles were rigidly connected to the rigid raft.

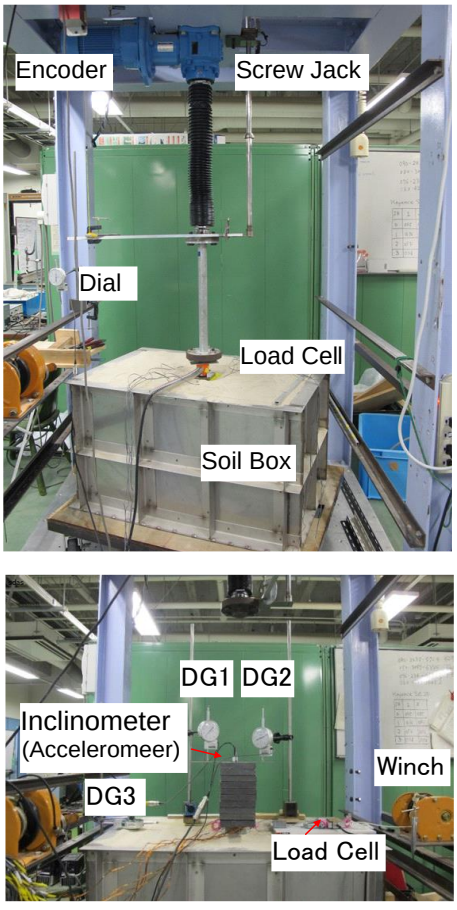

Fig. 2. Experiment setup: (a) vertical load test; (b) horizontal load test.

2.4 Test Procedure

For each model foundation, two cases were carried out. The first case was aimed to obtain the penetration resistance during PPT (Pile Penetration Test) and the bearing capacity of the foundation in VLT (Vertical Load Test). The second case was mainly aimed to obtain the performance of the foundation subjected to horizontal loading. In the 2nd case, HLT was carried out after PPT.

In PPT, the foundation was penetrated in the model ground using the screw jack (Fig. 2) until the pile embedment length reached 170 mm. After that, in the 1st case, VLT was conducted with the raft base being untouched to the ground surface (called PG stage or PG condition, PG: Pile group), as shown in Fig. 3. After the raft base touched the ground surface (called PR stage or PR condition, PR: Pile raft), VLT was again conducted. In the 2nd case, after the raft base touched the ground surface, the vertical load by screw jack was unloaded. HLT was carried out immediately after PPT. A death weight of 1000 N was placed on the foundation prior to the start of HLT, as shown in Fig. 2. Locations of open-ended pipe piles and plate piles are shown in Fig. 4.

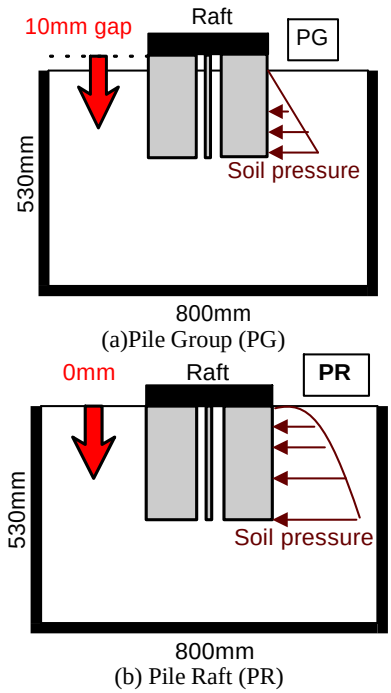

Fig. 3. Illustrations of load tests of PG and PR.

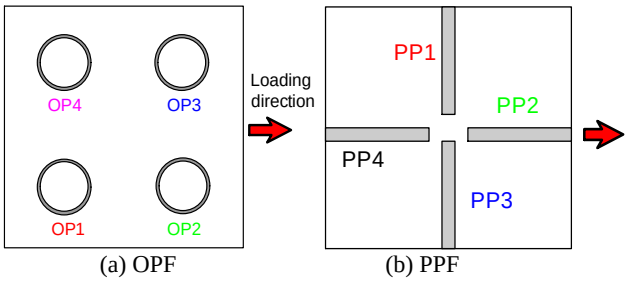

Fig. 4. Locations of piles in two foundations (top view).

After the completion of each experiment, cone penetration tests (CPTs) were conducted in the model ground. The cone used in CPTs had a diameter of 20.5 mm and an apex angle of 60 degrees. The diameter of the cone was similar with that of the model pipe pile. The results of CPTs showed that all the experiments were conducted under the same ground condition.

3 EXPERIMENT RESULTS

3.1 Results of PPT and VLT

Fig. 5 shows the relationships of the vertical load P and the settlement w of three model foundations during the PPT and VLT in the first cases. The results show that the load of open-ended pipe piles is around two times that of plate piles in the PPT and PG stages. However, in the PR stage, the loads of OP and PP are almost the same. This phenomenon will be discussed in detail later.

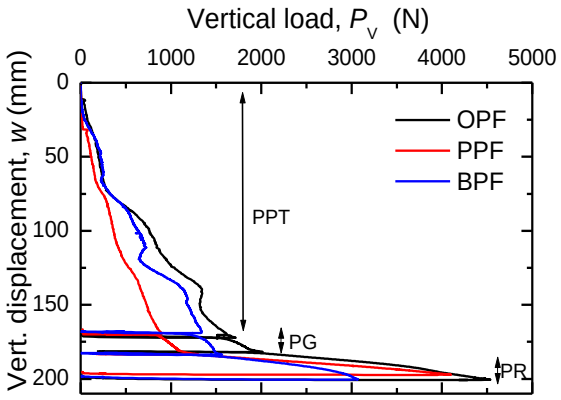

Fig. 5. Load settlement relations of foundations.

3.2 Results of VLT under PG and PR conditions

Fig. 6 shows comparisons of vertical load-settlement relationships of the foundations in stages of PG and PR. The vertical displacement, w, was zeroed at the start of VLT in Fig. 6. Loads of piles head were calculated from axial strain gauges. The loads carried by 4 OPs, 4 PPs and BP are also shown by the dashed lines. The difference between the total load and the pile load is the load carried by the raft. Note that the touchdown level of each foundation is different. It was intended to leave a gap of about 10 mm between the raft and the soil surface after the end of the PPT. However, due to the limited precision of the instrument, there was a difference of about 3 mm of the gap between three types of foundations prior to the start of VLT.

In the PG condition, of course, the load carried by piles was almost equal to the total load. The load of OPs was around two times that of PPs and 1.5 times that of BP. In the PR condition, the total loads of the foundations increased rapidly when the experimental stage turned to PR condition after the raft base touched the ground surface. It is interesting to notice that the loads of 4 OPs, 4 PPs and BP continued to increase in PR condition. However, the load of 4 PPs increased

significantly faster than that of 4 OPs or BP. The load of 4 PPs is only around 1000 N in the PG condition, while in the PR condition, this value became about 2.5 times when the settlement of the foundation reached about 27 mm.

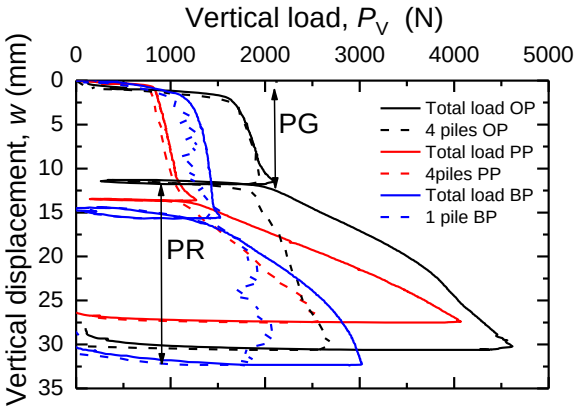

Fig. 6. Load-settlement relations of foundations on PG and PR.

A possible reason for this result is as follows. In the PR condition, because a part of vertical load is transferred to the ground through the raft base, stress levels in the soil surrounding the piles increase. Hence, the unit shaft resistance of the piles in PR condition increases compared to that in PG condition. Moreover, since the shaft area of PPs is the largest among the three model foundations, the increase in the shaft resistance (= the unit shaft resistance × the shaft area) of PPs is greater than that of OPs and BP in PR stage. As a result, the load carried by 4 PPs increased significantly faster than that carried by 4 OPs and BP under PR condition. The reason for this result will also be discussed in the numerical analyses later.

3.3 Results of HLT

HLT with a constant vertical load of 1000 N was conducted after the raft base touched the ground surface.

Fig. 7 shows horizontal load P_H vs. horizontal displacement u of OPF, PPF and BPF. It can be clearly seen from the figure that P_H of OPF is larger than that of PPF and BPF, and reached a peak at u = 12 mm. On the other hand, PPF carried the almost same horizontal load with OPF after u reached 12 mm and kept increasing. Among the three model foundations, the load of BPF was the smallest.

Fig. 8 shows horizontal displacement u vs. inclination θ of the raft in cases of OPF, PPF and BPF. It can be seen that the inclination of the raft in PPF is much smaller than that in OPF and BPF. It is thought that a high value of bending rigidity EI of PP2 and PP4 (strong axis, see Table 2 and Fig. 4) contributes to suppressing the inclination. Another reason is considered that even the bending rigidity EI of the whole (four) PPs including two PPs in weak axis and another two PPs in strong axis is smaller than that of BP, the greater distance between the front and the back edges of PPs can also contribute to preventing the foundation from rotating.

According to the results of experiments, it is found that the addition of piles to a raft increases the effective size of a foundation and can help resist horizontal load. This can also improve the performance of the foundation in reducing the amount of settlement and differential settlement, as well as increasing the ultimate load capacity.

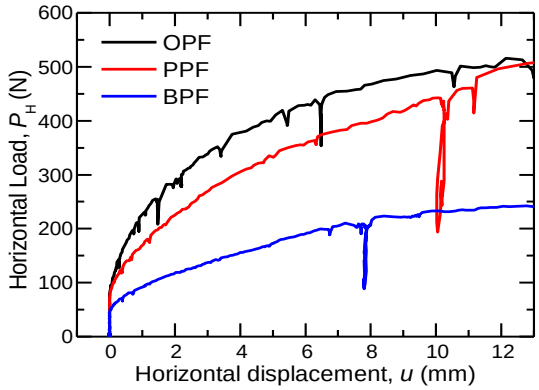

Fig. 7. Horizontal displacement vs. horizontal load.

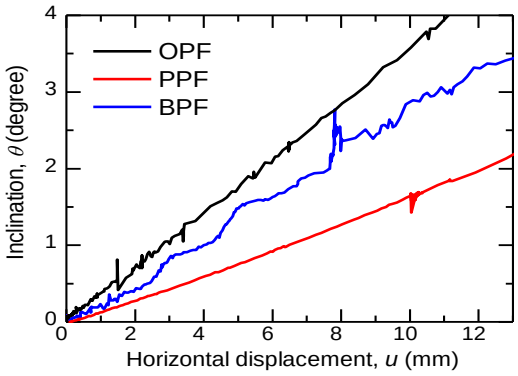

Fig. 8. Horizontal displacement vs. inclination.

4 NUMERICAL ANALYSES OF VERTICAL LOAD TESTS OF PPF

Behaviours of the sheet pile foundation model (PPF) subjected to vertical and horizontal loading were demonstrated in Section 3. In order to confirm the experimental results and to get more insight into the resistance mechanisms of the sheet pile foundation models, numerical analyses of the vertical load tests were conducted. A FEM software, PLAXIS 3D, was adopted to analyze the model load tests. The hypoplastic model, an incrementally nonlinear constitutive model, was employed to model the soil. The FEM results are presented and discussed in detail in comparison with the experimental results.

4.1 FEM simulation of the triaxial tests

To determine the soil parameters, element simulations of the triaxial CD tests on silica sand #6 were carried out. In triaxial CD tests (Vu et al, 2018), the

relative density of Silica sand #6 was the same with that of the model ground in this research.

The results of the simulations are shown in Fig. 10. And the soil parameters used in the simulations are listed in Table 3. The calculated results well simulated the overall trend of the measured results.

Table 3. Parameters of the hypoplastic model (after Tuan, 2018).

Property	Value
Critical friction angle, φ_c (deg.)	31
Granular hardness, h_s (N/mm^2)	6000
Exponential factor, n	0.26
Lower limit of void ratio, e_{d0}	0.663
Critical voil ratio, e_{c0}	1.1
Upper limit of void ratio, e_{i0}	1.2
Exponential factor, α	0.14
Exponential factor, β	1.4
Stiffness multiplier for initial and reverse loading, m_R	5
Stiffness multiplier for neutral loading, m_T	2
Small strain stiffness limit, R_{max}	1×10^{-4}
Stiffness reduction parameter, β_r	0.5
Stiffness reduction parameter, χ	2
Shift of mean stress due to cohesion, p_t	5×10^{-3}
Initial void ration, e	0.739

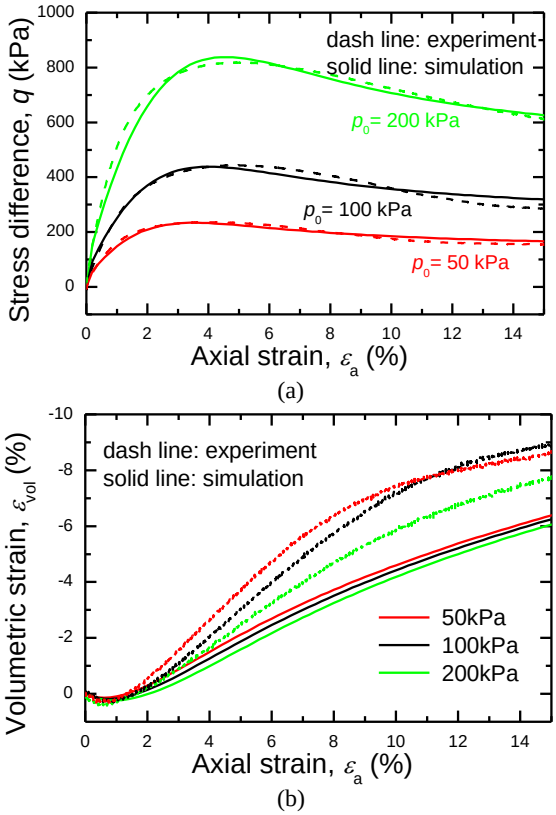

Fig. 9. (a) Stress difference q versus axial strain ε_a; (b) Volumetric strain ε_{vol} versus axial strain ε_a

Particularly, it is seen from Fig. 9(b) that the calculated results were in good agreement with the tendency of the measured dilatancy behaviours. Therefore, the parameters shown in Table 3 were used to simulate the model tests.

4.2 Numerical model of PPF and simulation procedure

In the numerical modelling, the raft was modeled by a linear elastic material, and the properties of the raft are shown in Table 4.

To model the plate pile, a hybrid model for pipe piles (Kimura and Zhang, 2000) was referred. In this study, a hybrid model in which plate elements are surrounded by solid volume elements was proposed. Fig. 10 shows the hybrid model for plate piles of this research. The plate element carried a large proportion (90%) of the bending stiffness EI and axial stiffness EA of the pile. Therefore, the stiffness of the surrounding volume elements is reduced to 10% of the actual value. However, it is noticed that the reduced stiffness of the surrounding elements of the hybrid pile is still much higher than that of the surrounding soil. The properties of the plate and the solid pile are summarized in Table 4.

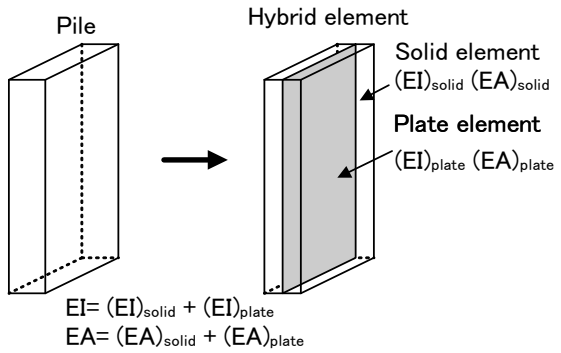

Fig. 10. Mechanism of the hybrid model of plate pile.

Table 4. Properties of the elastic elements

Description	Plate	Solid pile	Raft
Material model		linear elastic	linear elastic
Unit weight, γ (N/mm^3)	2.586×10^{-5}	2.586×10^{-5}	3.392×10^{-5}
Young's modulus, E (N/mm^2)	64.17×10^{3}	7.13×10^{3}	71.3×10^{3}
Poisson's ratio, ν	-	0.343	0.3

To model the soil-pile interface, a series of direct shear tests between the pile and the sand were conducted to estimate the interface friction angle $\phi_{p\text{-}s}$, and it was set 32.09° in simulation. One-dimensional modulus E_{oed}^{ref} and the interface cohesion were set as 600 N/mm^2 and 0.0065 N/mm^2, which were determined by fitting the result of VLT on single plate pile.

As shown in Fig. 11, only a half of the foundation and the ground was modelled due to symmetric condition. In this study, VLT on single plate pile was first calculated to determine the parameters of interface. After that, the VLT of PG and PR were analyzed. The calculation

procedure was the same as the experimental procedure, which was as follows: First self-weight analysis of the model ground alone was conducted; after that the raft and the piles were set in the ground; finally, the VLT of single pile, PG or PR was simulated by applying a prescribed displacement.

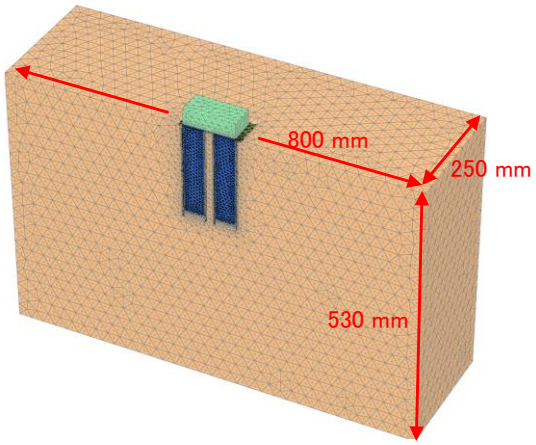

Fig. 11. Finite element mesh of the numerical models.

4.3 Results of numerical analyses on PPF

Fig. 12 shows that the calculated results of single pile are in good agreement with the measured results. The trend of the measured result was reasonably simulated. The yielding point was observed at a settlement of around 0.5 mm in the measured result, and this settlement was also well simulated. The initial stiffness (for the settlement smaller than around 0.25 mm) in the calculation was almost identical with the measured one. As the settlement increased from 0.25 mm to 0.5 mm, the calculated stiffness decreased faster than the measured result, which led to the underestimation of the yielding load.

Regarding the bearing capacity of the single pile, Fig. 12(a) shows that the calculated result at pile head displacement w_H= 5 mm is smaller than the measured one except for the case when E_{oed}^{ref} is 600 N/mm^2 and c_{inter} is 0.007 N/mm^2. Since the calculated bearing capacity of single pile continually increased with the increase in pile head displacement, c_{inter} = 0.0065 N/mm^2 was selected in the simulation of PG and PR. Fig. 12(b) shows that the bearing capacity of the single pile increased with the E_{oed}^{ref} increased.

Fig. 13 shows measured and calculated load-settlement relationships in the cases of the plate pile foundation (PG and PR). Considering the tendency of initial stiffness first, Fig. 13 shows that the calculated results were in qualitative agreement with the measured results. Both the measured and calculated results show that the pile group resistance almost reached the peak at a settlement of 1.5 mm. It is seen that the trends of measured load-settlement curves are simulated reasonably in FEM calculation, in which the PR have much higher resistance and stiffness than those of the corresponding PG.

Fig. 14 shows horizontal stress σ_{xx} in the ground at w = 10 mm. It can be found that the pressure transferred from the raft base to the ground in the case of PR significantly increased the stress level of soil around the piles, resulting in the increase in stiffness and strength of soil, leading to the larger pile resistance of PR compared with that in PG. These calculated results verified the discussion about difference between PG and PR in Section 3.2.

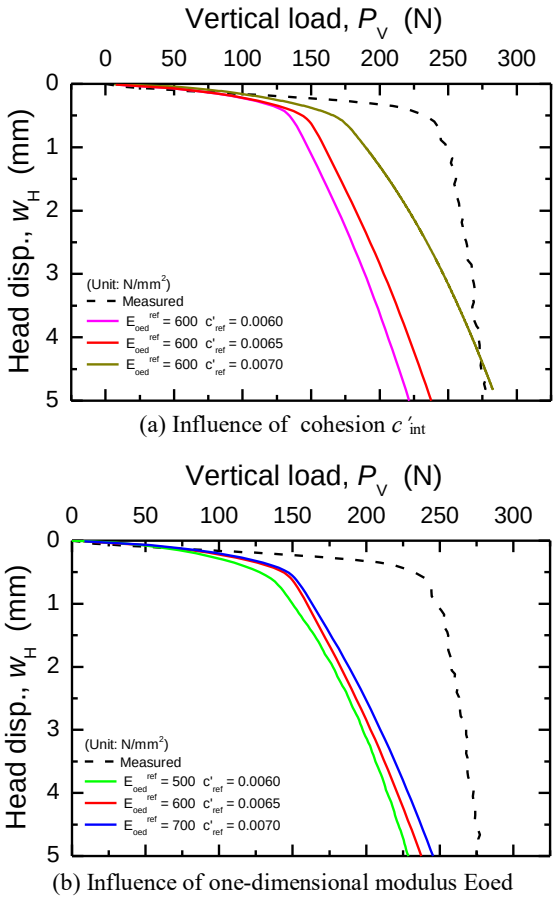

Fig. 12. Measured and calculated results during SLTs of SP.

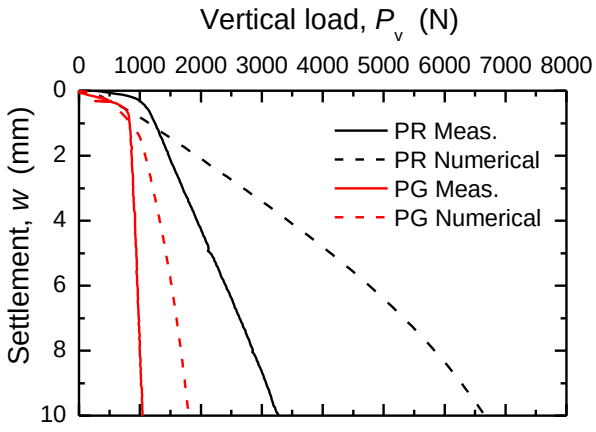

Fig. 13. Measured and calculated results during SLTs of PPF.

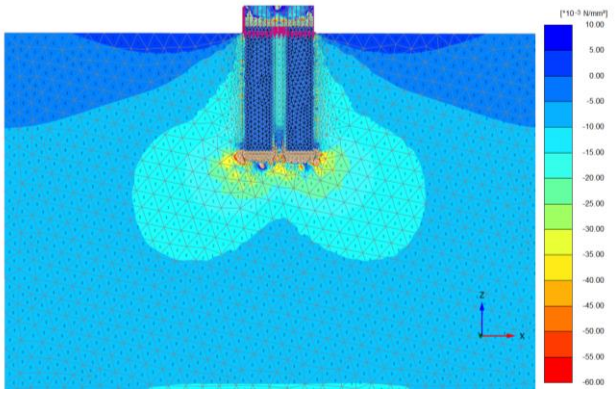

(a) PG

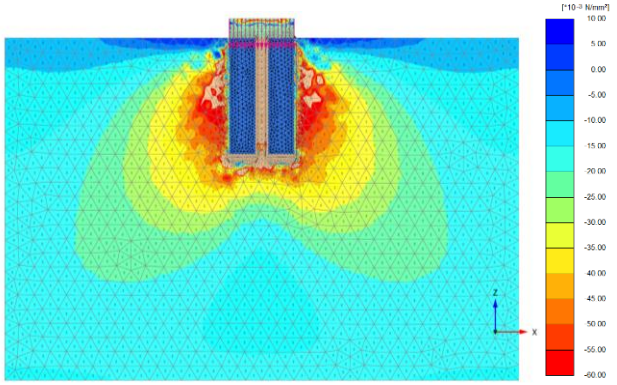

(b) PR

Fig. 14. Horizontal stress σ_{xx} in the ground at w = 10 mm from FEM analysis of PG and PR (from 10×10^{-3} to -60×10^{-3}, unit: N/mm^2).

CONCLUDING REMARKS

In this research, a series of model experiments were conducted to explore the load transfer behaviours of piled foundations supported by OPs, PPs or BP in dry sand ground subjected to vertical and horizontal loading. And the FEM analyses of VLT on PPF were also conducted. Interesting findings from this experimental and numerical study are as follows:

(1) In vertical loading, the vertical resistance of OPs was around two times that of PPs and 1.5 times that of BP in PG condition. Under PR condition, the vertical load of PPF increased faster than other two model foundations.

(2) In horizontal loading, the horizontal resistance of BPF is the smallest among three model foundations. P_H of PPF tended to increase continuously, and PPF carried the almost same horizontal load as OPF after u reached 12 mm.

(3) The FEM calculation results of PPF under PG and PR conditions were in qualitative agreement with the measure results. The effect of raft on the bearing capacity was also verified by comparing the horizontal stress of soil around the piles in PG and PR, which was not measured in the experiment.

In summary, PPF can carry almost the same load as OPF under both vertical and horizontal loading conditions. Sheet pile foundation would be a promising alternative to conventional round pipe pile foundation, especially in high-seismic areas where foundations will experience both vertical and horizontal loading. Moreover, the numerical method proposed in this paper could be used in the design of piled raft foundation supported by sheet piles.

ACKNOWLEDGEMENTS

The authors would like to express our appreciation to Mr. Shinya Shimono, technician of Kanazawa University, for his technical support in this study.

REFERENCES

1) Punrattanasin, P., Kusakabe, O., Murate, O., Koda, M. and Nishioka, H. (2002): Sheet Pile Foundation on Sand Under Combined Loading - a Literature Review and Pre liminary Investigation. *Technical Report of Tokyo Institute of Technology*, 65, 57-85.

2) Kusakabe, O., Ueno, K., and Ishihara, Y. (Eds.). (2018): *Proceedings of the Second International Conference on Press-in Engineering 2018*, Kochi, Japan.

3) Vu, A.T., Matsumoto T., Kobayashi, S. and Nguyen, T. L. (2018): Model load tests on battered pile foundations and finite-element analysis. *Int. Journal of Physical Modelling in Geotechnics*, 18(1), 33-54.

4) Kimura, M. and Zhang F. (2000): Seismic evaluations of pile foundations with three different methods based on three-dimensional elasto-plastic finite element analysis, *Soil and Foundation*, 40(5), 113-132.